Do current cosmological observations rule out all covariant Galileons?

Simone Peirone,[1] Noemi Frusciante,[2] Bin Hu,[3] Marco Raveri,[4,1] and Alessandra Silvestri[1]

[1]*Institute Lorentz, Leiden University, P.O. Box 9506, Leiden 2300 RA, The Netherlands*
[2]*Instituto de Astrofisica e Ciências do Espaço, Faculdade de Ciências da Universidade de Lisboa, Edificio C8, Campo Grande P-1749016, Lisboa, Portugal*
[3]*Department of Astronomy, Beijing Normal University, Beijing 100875, China*
[4]*Kavli Institute for Cosmological Physics, Enrico Fermi Institute, The University of Chicago, Chicago, Illinois 60637, USA*

We revisit the cosmology of covariant Galileon gravity in view of the most recent cosmological data sets, including weak lensing. As a higher derivative theory, covariant Galileon models do not have a ΛCDM limit and predict a very different structure formation pattern compared with the standard ΛCDM scenario. Previous cosmological analyses suggest that this model is marginally disfavored, yet cannot be completely ruled out. In this work we use a more recent and extended combination of data, and we allow for more freedom in the cosmology, by including a massive neutrino sector with three different mass hierarchies. We use the Planck measurements of cosmic microwave background temperature and polarization; baryonic acoustic oscillations measurements by BOSS DR12; local measurements of H_0; the joint light-curve analysis supernovae sample; and, for the first time, weak gravitational lensing from the KiDS Collaboration. We find, that in order to provide a reasonable fit, a nonzero neutrino mass is indeed necessary, but we do not report any sizable difference among the three neutrino hierarchies. Finally, the comparison of the Bayesian evidence to the ΛCDM one shows that in all the cases considered, covariant Galileon models are statistically ruled out by cosmological data.

I. INTRODUCTION

Covariant Galileon (CG) models [1] are a class of scalar-tensor theories belonging to the broader class of generalized Galileons, i.e. scalar-tensor theories with second order equations of motion [2,3]. Galileon theories have gained interest in recent years because they allow for self-accelerating solutions that could describe both the inflationary epoch and the late time accelerated expansion [4–7].

Along with a modification of the background expansion history, CG models lead to peculiar features in the large scale structure [8–10], in particular contributing to enhancing the low-ℓ part of the cosmic microwave background (CMB) lensing spectrum. Quartic and quintic models (namely those including terms up to quartic and quintic order in the scalar field, respectively) are preferred by Planck data because they predict a lower impact of the integrated Sachs-Wolfe (ISW) effect, but at the same time it is hard for them to pass the Solar System constraints, which are better accommodated by the cubic model (as previously, this model contains three copies of the scalar field). Moreover, as shown in [9], the CG model prefers nonzero neutrino masses at over 5σ, which in turn affect the H_0 estimation, making it compatible with local measurements.

In this paper we analyze the cosmology of CG models in light of the current cosmological observations, including,

for the first time, data from the weak gravitational lensing (WL) survey of KiDS [11–13]. Previous works [8–10] have shown that for the CG model it is hard to provide a fit to data better than the standard cosmological model and a recent analysis showed indeed that the cubic branch can be ruled out at 7.8σ with data including CMB, baryonic acoustic oscillations (BAO) and ISW. However the quartic and quintic models cannot be completely excluded by such a collection of data. In this work, we extend the analysis by using more recent data sets and adding the WL measurements, simultaneously allowing for different mass hierarchies in the massive neutrinos sector.

The cosmological impact of the mass hierarchy has not been explored extensively. In general, it is expected that the sensitivity to the type of hierarchy increases as the bound on the total mass of neutrinos becomes tighter; see e.g. [14]. Only very recently has it been shown that in the ΛCDM scenario there is a mild preference for the normal hierarchy [14–16] and that, in models with a parametrized dark energy equation of state, different hierarchies seem to have a slight impact on the dark energy parameters while leaving unaffected the standard cosmological parameters [17]. Additionally, the different hierarchies imply different transition redshifts from relativistic to nonrelativistic regimes, and this would leave an impact on the matter power spectrum. Such an effect has been usually neglected,

because it is negligible if compared to the effect coming from the the total neutrino mass. However, data coming from the last generation of surveys and future experiments, such as EUCLID, might have the accuracy needed to constraint these features [18].

Furthermore, the inclusion of new parameters, such as the parameters specific to the CG model or to the neutrinos sector, could allow us to ease the tensions between CMB measurements and low redshift data, concerning both the local measurements of the Hubble constant as well as WL measurements. The first-year results from the DES Collaboration [19,20] show that the CMB-WL tension on $S_8 = \sigma_8 \sqrt{\Omega_m/0.3}$ is somehow reduced from 2.3σ (KiDS vs Planck) to 1.6σ (DES vs Planck). Similarly, also the CMB-H_0 tension seems to be reduced by the DES measurements, relying on the large error bars of the first-year release. While these are barely statistically significant, and likely to be settled, it is still interesting to investigate them within the framework of extended models such as the CG. The use of WL data, a novel aspect of our analysis, has a relevant role in studying the CMB-WL tension.

Finally, the recent multimessenger observation of the binary neutron star merger [21–23] was shown to cast stringent constraints on the quartic and quintic Galileon Lagrangians, practically ruling them out as dark energy candidates [24–28]. In this work we use a complementary and entirely independent set of data, from cosmological observations, and derive very stringent constraints on all three CG Lagrangians.

The manuscript is organized as follows. In Sec. II, we review the CG model with its background evolution when a tracker solution is considered and we summarize the definitions of the neutrino hierarchies. In Sec. III, we introduce the Einstein Boltzmann code and the data sets used for the analysis. In Sec. IV, we discuss the results and in Sec. V, we draw our conclusions.

II. THE MODEL

A. Covariant Galileons

The Galilean symmetry $\partial_\mu \phi \rightarrow \partial_\mu \phi + b_\mu$ (with b_μ a constant) has been considered to construct the most general action with a metric ($g_{\mu\nu}$) and a scalar field (ϕ), whose field equations include up to second order derivatives [29], thus avoiding Ostrogradski instabilities [30]. The first formulation was in flat space and the generic structure of the Galileon Lagrangian terms follows $\partial \phi \cdot \partial \phi (\partial^2 \phi)^{n-2}$, up to $n = 5$, as higher order Lagrangians are just total derivatives. The same approach has been generalized on a curved space-time, but in this case, in order to retain second order field equations and ensure the propagation of only one additional degree of freedom, extra terms nonminimally coupled to the metric have been added to the action [1]. This ended up with the loss of the Galileon symmetry, while preserving the shift symmetry. The resulting model is known as CG and the action reads

$$
\begin{aligned}
S_{CG} = \int d^4x \sqrt{-g} \bigg\{ &\frac{m_0^2}{2} R - \frac{1}{2} c_2 X + \frac{c_3}{M^3} X \Box \phi \\
&+ \frac{c_4}{4M^6} X^2 R - \frac{c_4}{M^6} X[(\Box\phi)^2 - \phi^{;\mu\nu} \phi_{;\mu\nu}] \\
&+ \frac{3c_5}{4M^9} X^2 G_{\mu\nu} \phi^{;\mu\nu} + \frac{c_5}{2M^9} X[(\Box\phi)^3 \\
&- 3\Box\phi \phi^{;\mu\nu} \phi_{;\mu\nu} + 2\phi^{;\mu\nu} \phi_{;\mu\sigma} \phi_{;\sigma}^{;\nu}] \bigg\},
\end{aligned}
\tag{1}
$$

where m_0^2 is the Planck mass, g is the determinant of the metric, R and $G_{\mu\nu}$ are respectively the Ricci scalar and the Einstein tensor, $X = \phi^{;\mu} \phi_{;\mu}$ is called the kinetic term and $\{;\}$ stands for the covariant derivative. Moreover, c_i are constant dimensionless parameters and $M^3 = m_0 H_0^2$, with H_0 being the present time value of the Hubble parameter.

In order to investigate the reliability of this model on cosmological linear scales, we will exploit the tracker solution for the background evolution [31]. The tracker solution relates the scalar field and the Hubble parameter as follows:

$$
\left(\frac{\mathcal{H}}{a}\right)^2 \psi = \xi H_0^2 = \text{const},
\tag{2}
$$

where $\psi = \frac{1}{m_0} \frac{d\phi}{d\ln a}$ is a dimensionless field, ξ is a dimensionless constant and $\mathcal{H} \equiv \frac{da}{ad\tau}$ is the conformal Hubble parameter. Then, Eq. (2) can be used to obtain the expansion history $\mathcal{H}$ along the tracker [9]. Indeed, assuming the tracker solution and a flat Friedmann-Lemaître-Robertson-Walker metric with signature $(-, +, +, +)$, the modified Friedmann equation can be written as follows:

$$
\begin{aligned}
E^4(a) = E^2(a) \bigg(&\Omega_{m,0} a^{-3} + \Omega_{r,0} a^{-4} + \Omega_{\nu,0} \frac{\rho_\nu(a)}{\rho_{\nu,0}} \bigg) \\
&+ \left[\frac{c_2}{6} \xi^2 + 2c_3 \xi^3 + \frac{15}{2} c_4 \xi^4 + 7c_5 \xi^5 \right],
\end{aligned}
\tag{3}
$$

where $E = \frac{\mathcal{H}}{aH_0}$ and $\Omega_{i,0}$ stand for the present density parameters for baryons and cold dark matter ($m = b$, cdm), radiation and massless neutrinos (r) and massive neutrinos (ν). Then, Eq. (3) can be solved to get $\mathcal{H}$. Along with this equation, one has to consider two further constraints: one comes from the flatness condition, which immediately gives the definition of the present density parameter for the scalar field,

$$
\Omega_{\phi,0} = \frac{c_2}{6} \xi^2 + 2c_3 \xi^3 + \frac{15}{2} c_4 \xi^4 + 7c_5 \xi^5,
\tag{4}
$$

and the second is obtained by combining the equation for the scalar field (obtained by varying the action with respect to the scalar field) and Eq. (2), which gives

$$c_2\xi + 6c_3\xi^2 + 18c_4\xi^3 + 15c_5\xi^4 = 0. \qquad (5)$$

Finally, to avoid scaling degeneracy one has the freedom to fix $c_2 = -1$ without loss of generality.

In the present work, we will analyze three subclasses of the CG model and the constraints (4)–(5) will be used to define the corresponding sets of free parameters as follows:

(i) G_3: Cubic model, $c_3 \neq 0$, $\{c_4, c_5\} = 0$. Using the constraint relations, one has

$$\xi = \sqrt{6\Omega_{\phi,0}}, \qquad c_3 = \frac{1}{6\sqrt{6\Omega_{\phi,0}}}. \qquad (6)$$

Thus, in this case the number of free parameters is the same as in ΛCDM.

(ii) G_4: Quartic model, $\{c_3, c_4\} \neq 0$, $c_5 = 0$. We have

$$c_3 = \frac{1}{2}\xi^{-1} - 2\Omega_{\phi,0}\xi^{-3}, \qquad (7)$$

$$c_4 = -\frac{1}{9}\xi^{-2} + \frac{2}{3}\Omega_{\phi,0}\xi^{-4}, \qquad (8)$$

with one extra free parameter ξ.

(iii) G_5: Quintic model, $\{c_3, c_4, c_5\} \neq 0$.
    Solving Eqs. (4)–(5) for c_4 and c_5, one gets

$$c_5 = \frac{4}{3}\Omega_{\phi,0}\xi^{-5} + \frac{1}{3}c_2\xi^{-3} + \frac{2}{3}c_3\xi^{-2},$$

$$c_4 = -\frac{10}{9}\Omega_{\phi,0}\xi^{-4} - \frac{1}{3}c_2\xi^{-2} - \frac{8}{9}c_3\xi^{-1}. \qquad (9)$$

Then, one has $\{\xi, c_3\}$ as extra free parameters.

B. Mass hierarchies

It is well known that the mass of neutrinos leaves clear signatures on cosmological observables [32], such as a modification of the time at which matter-radiation equality occurs, causing shifts of the first peak of the CMB temperature and polarization power spectra, via the early integrated Sachs-Wolfe (eISW) effect; massive neutrinos also cause the free streaming of density perturbations on small scales, while behaving like clustering cold dark matter on larger scales. Cosmological analyses have established robust upper limits on the sum of the neutrino masses of $\Sigma m_\nu < 0.13$ eV [33], $\Sigma m_\nu < 0.12$ eV [34] and very recently $\Sigma m_\nu < 0.20$ eV [20] at a 95% confidence level. Measurements of neutrino flavor oscillations imply that at least two neutrino species have nonzero masses [35] and the differences of the square of the neutrino masses are $\Delta_{12}^2 = m_2^2 - m_1^2 = 7.5 \times 10^{-5}$ eV^2, from which it follows $m_2 > m_1$ and $|\Delta_{31}^2| = |m_3^2 - m_1^2| = 2.5 \times 10^{-3}$ eV^2, with m_i being the mass of the ith massive eigenstate. Since such experiments can just measure their differences, we are left with three possible mass hierarchies: the *normal hierarchy*,

when m_3 is taken to be the largest mass $m_3 \gg m_2 > m_1$; the *inverted hierarchy*, when m_3 is considered the smallest $m_2 > m_1 \gg m_3$; and in the final option, the *degenerate hierarchy*, each mass is orders of magnitude bigger than each mass splitting ($m_j \sim m_i \gg \Delta_{ij}$). Thus, all three species are treated as having effectively the same mass $m_1 = m_2 = m_3$.

In the present analysis we allow for different mass hierarchies. This will permit us to investigate possible effects due to the different free streaming length scales associated to the three neutrino masses and to see if the current cosmological data have the sensitivity to capture this effect. Moreover, the additional freedom connected to the choice of the hierarchy can be essential in order to make the CG models' predictions compatible with data.

III. METHOD

A. EFTCAMB

We perform the present analysis by making use of EFTCAMB/EFTCosmoMC[1] [36,37]. These patches have been obtained by implementing the effective field theory approach for dark energy and modified gravity (hereafter EFT) [38–44] into CAMB/CosmoMC [45,46].

In order to implement a specific model in EFTCAMB one has to implement the background evolution and provide a mapping between the free EFT functions $\{\Omega(a), \gamma_i(a)\}$, with $i = 1...6$, and the model [38–41,44,47,48]. In the case under analysis, we have implemented the background evolution as in Eq. (3) and worked out the mapping as follows:

$$\Omega = \frac{a^4}{2\mathcal{H}^4}H_0^4\xi^4\left[c_4 - 6c_5\xi\left(1 - \frac{\dot{\mathcal{H}}}{\mathcal{H}^2}\right)\right],$$

$$\gamma_1 = \frac{a^2 H_0^2\xi^3}{4\mathcal{H}^2}\left[2c_4\xi\left(24 - \frac{\ddot{\mathcal{H}}}{\mathcal{H}^3} - 9\frac{\dot{\mathcal{H}}}{\mathcal{H}^2} + 5\frac{\dot{\mathcal{H}}^2}{\mathcal{H}^4}\right)\right.$$
$$+ 3c_5\xi^2\left(12 + 10\frac{\ddot{\mathcal{H}}}{\mathcal{H}^3} + 21\frac{\dot{\mathcal{H}}}{\mathcal{H}^2} + \frac{\ddot{\mathcal{H}}}{\mathcal{H}^4} - 50\frac{\dot{\mathcal{H}}^2}{\mathcal{H}^4}\right.$$
$$\left.+ 42\frac{\dot{\mathcal{H}}^3}{\mathcal{H}^6} - 18\frac{\dot{\mathcal{H}}}{\mathcal{H}^2}\frac{\ddot{\mathcal{H}}}{\mathcal{H}^3}\right) + 2c_3\left(4 - \frac{\dot{\mathcal{H}}}{\mathcal{H}^2}\right)\right],$$

$$\gamma_2 = -\frac{a^3 H_0^3\xi^3}{\mathcal{H}^3}\left[c_5\xi^2\left(3 + 3\frac{\ddot{\mathcal{H}}}{\mathcal{H}^3} + 24\frac{\dot{\mathcal{H}}}{\mathcal{H}^2} - 18\frac{\dot{\mathcal{H}}^2}{\mathcal{H}^4}\right)\right.$$
$$\left.- 2\xi c_4\left(\frac{\dot{\mathcal{H}}}{\mathcal{H}^2} - 7\right) + 2c_3\right],$$

$$\gamma_3 = -\frac{a^4}{\mathcal{H}^4}H_0^4\xi^4\left(2c_4 + 3c_5\xi\frac{\dot{\mathcal{H}}}{\mathcal{H}^2}\right), \qquad (10)$$

where dots stand for derivatives with respect to conformal time, τ. Finally, we have $2\gamma_5 = -\gamma_4 = \gamma_3$ and $\gamma_6 = 0$.

---

[1]EFTCAMB webpage: http://www.eftcamb.org.

We impose flat priors over the range [0, 10] for the model parameters c_3 and ξ (when needed) and a flat prior over [0, 1] eV for Σm_ν, when not set to zero.

Finally, the implementation of the CG models in EFTCAMB has been compared with other Einstein-Boltzmann solvers for modified gravity in a recent work [49], showing subpercent agreement at all scales of interest. It demonstrates that the EFT approach is very robust to recover the linear perturbation theory from the covariant approach.

B. Data sets

In the present analysis we consider the Planck measurements [50,51] of CMB temperature and polarization on large angular scales, limited to multipoles $\ell < 29$ (low-ℓ Temperature and Polarization likelihood) and the CMB temperature on smaller angular scales [PLIK Temperature-Temperature(TT) likelihood, $30 < \ell < 2508$] along with BAO measurements of the BOSS DR12 (*consensus release*) [52]. For the Planck likelihood, we also vary the nuisance parameters that are used to model foregrounds as well as instrumental and beam uncertainties. We shall refer to this data set as PB (Planck + BAO). We then complement it with results from local measurements of H_0 [53], weak gravitational lensing from the KiDS Collaboration [11–13,54] and the joint light-curve analysis (JLA) supernovae (SN) sample, as introduced in Ref. [55]. For the weak lensing data set, we decide to perform a cut at nonlinear scales, since the predictions for CG models at those scales are not known very precisely. For this reason, we follow the analyses done in Refs. [56,57], with the cut in the radial direction $k \leq 1.5\,h\,\mathrm{Mpc}^{-1}$ and where the contribution from the ξ^- correlation function is removed. In this way the analysis has been shown to be sensitive to the linear scales only (see Fig. 2 of [57]). We shall refer at this second data set as PBHWS, i.e. Planck + BAO + H_0 + WL + SN. This is the first time CG theories are being analyzed against such a wide data set, containing weak gravitational lensing data from KiDS.

IV. RESULTS AND DISCUSSION

We analyze the three different CG models (i.e. G_3, G_4 and G_5) within four different cosmological scenarios, namely massless neutrinos and massive neutrinos with the three different hierarchies: normal, inverted and degenerate. We will always report also the results for the fiducial ΛCDM cosmology; thus, we will analyze a total of 16 different scenarios within the two data sets described in Sec. III B.

In Figs. 2, 3 and 4, we show the joint marginalized posterior distributions of the cosmological parameters σ_8, Ω_m, H_0, and Σm_ν, along with the model parameters ξ and c_3, obtained through the analysis of the G_3, G_4 and G_5 models for all four neutrino configurations. For comparison with the CG results, in Fig. 1 we show the posterior distributions of the ΛCDM model.
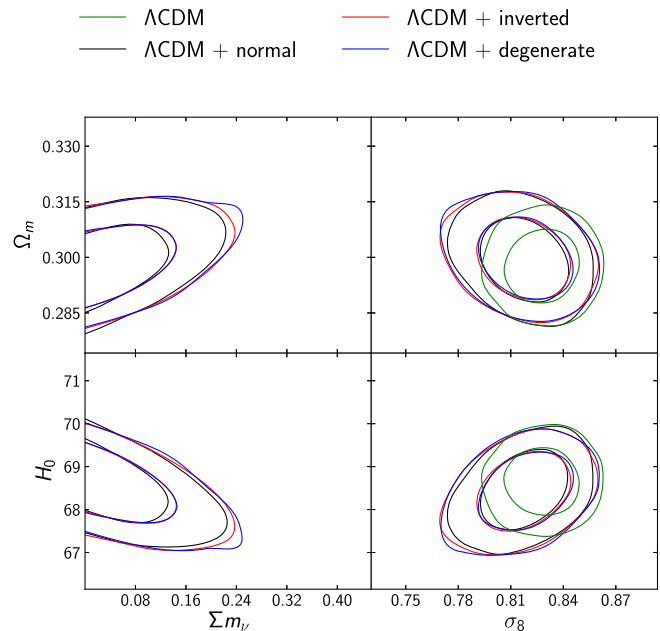

FIG. 1. The joint marginalized posterior of ΛCDM runs with the PBHWS data set. The lines correspond to the 68% C.L. and 95% C.L. regions. Different colors correspond to different neutrino scenarios as stated in the legend.

Let us first consider the case of zero neutrino mass and focus on the effects that the scalar field of CG models has on the cosmological parameters. The density parameter of baryons and cold dark matter, Ω_m, is shifted towards lower
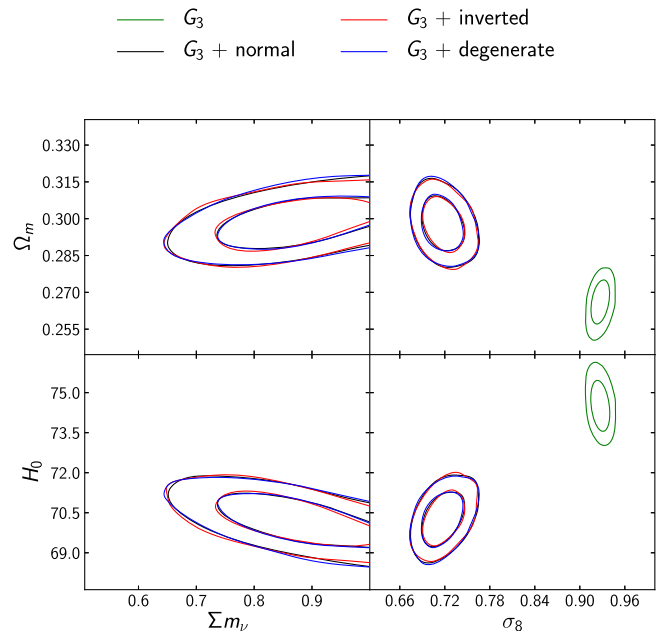

FIG. 2. The joint marginalized posterior of G_3 runs with the PBHWS data set. The lines correspond to the 68% C.L. and 95% C.L. regions. Different colors correspond to different neutrino scenarios as stated in the legend.
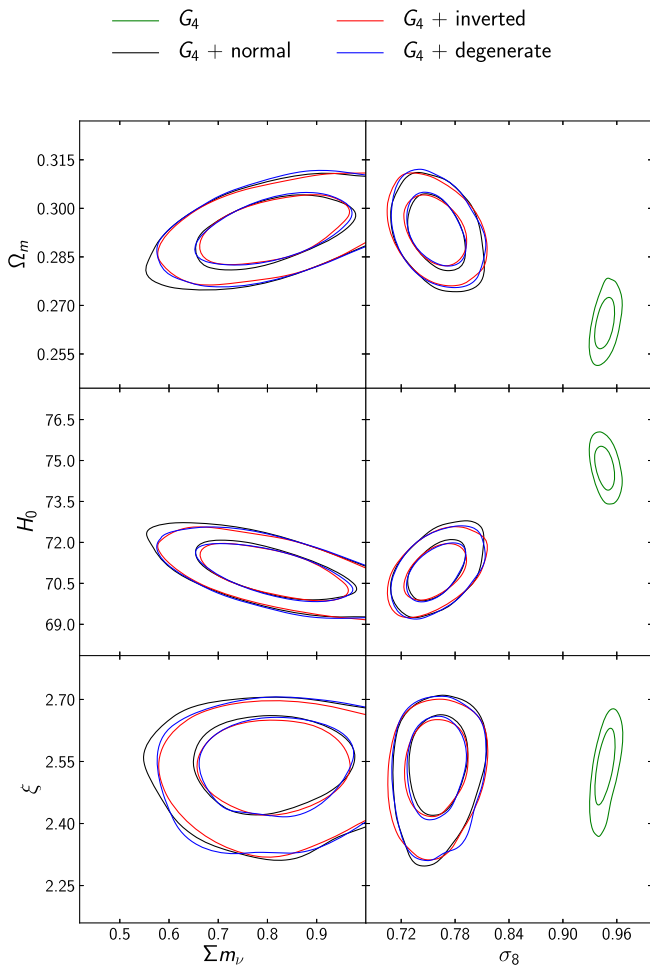
FIG. 3. The joint marginalized posterior of G_4 runs with the PBHWS data set. The lines correspond to the 68% C.L. and the 95% C.L. regions. Different colors correspond to different neutrino scenarios as stated in the legend.
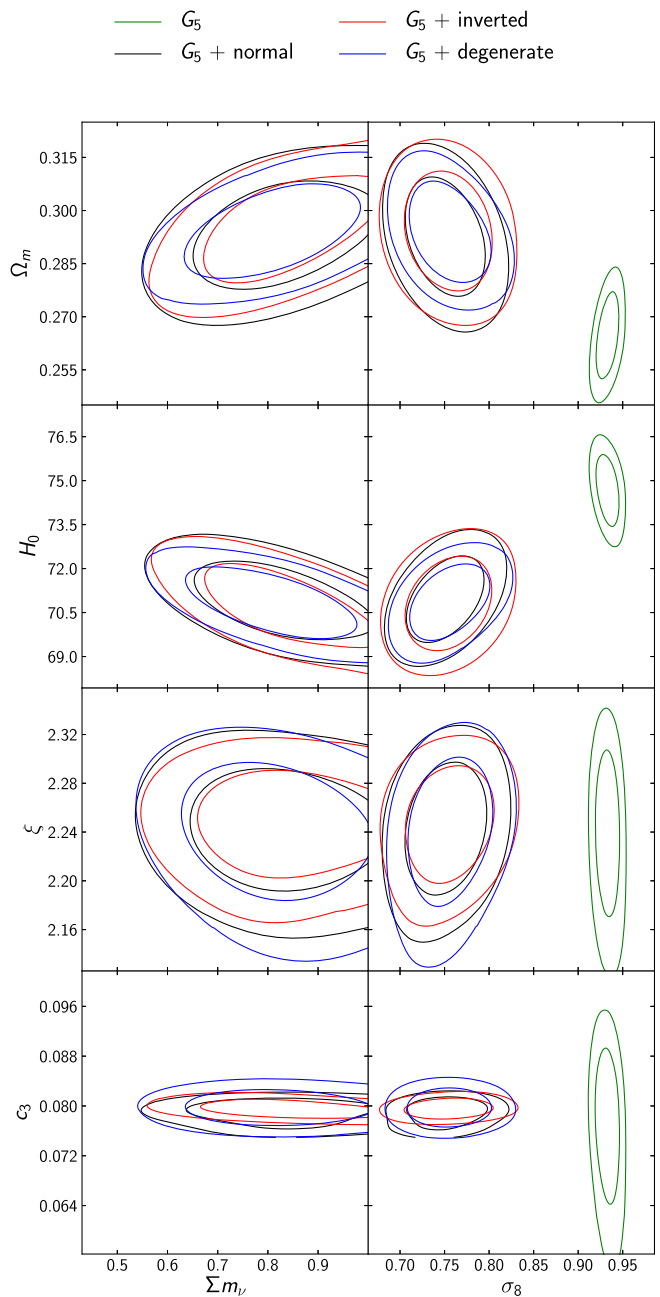

FIG. 4. The joint marginalized posterior of G_5 runs with the PBHWS data set. The lines correspond to the 68% C.L. and the 95% C.L. regions. Different colors correspond to different neutrino scenarios as stated in the legend.

values in the CG cosmologies; on the contrary, σ_8 increases. From the different plots we can also see that the value of H_0 is enhanced, easing the tension between CMB and the local measurements of H_0. Furthermore, we notice that there is no substantial impact of the different data sets on these parameters; then in the figures we show only the results obtained with the full PBHWS data set.

We then open the massive neutrino sector. As already noticed in Ref. [58], all CG cosmologies are compatible with a detection of the neutrino mass ($\Sigma m_\nu \neq 0$). In general, the value of Σm_ν for the CG cosmologies is higher (a factor of 10) if compared to the ΛCDM model best fit; see Table II. The cosmological parameters turn out to be affected by the presence of massive neutrinos, as expected, but the different hierarchies do not lead to a noticeable difference either on the cosmological or on the model parameters. The effect of the massive neutrinos on H_0 is to contrast the impact of the scalar field; overall the value of H_0 in those runs remains higher compared to the ΛCDM one, but still compatible within 2σ error bars. Ω_m increases

to higher values with respect to the zero neutrino mass cases, being now compatible with the ΛCDM case. As a consequence, σ_8 assumes lower values with respect both to the zero neutrino mass CG cosmologies and the four ΛCDM scenarios. σ_8 assumes the lowest values for the G_3 case. The model parameter ξ in G_4 and G_5 is not affected by the inclusion of massive neutrinos and, in general, in G_5 it assumes lower values. Finally, the values of c_3 in G_5, in all four scenarios, are compatible within the
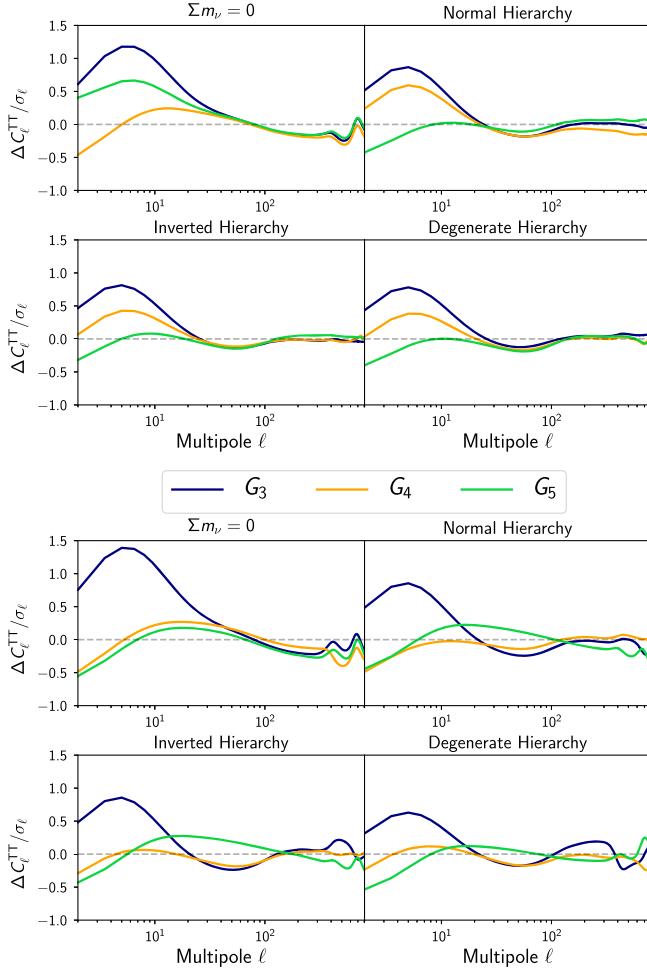
FIG. 5.   Deviation in the CMB TT power spectra in units of TT variance, $\sigma_\ell = \sqrt{2/(2\ell+1)}C_\ell^{\Lambda\mathrm{CDM}}$, for best fit parameters for PB (top) and PBHWS (bottom), computed with respect to ΛCDM.

errors; thus, the mean value of c_3 is not affected by the introduction of massive neutrinos, while its error bars are larger in the massless neutrinos scenario.

The impact of the two different data sets is to move to slightly bigger values of Σm_ν in the PBHWS with respect to PB. This has the effect of reducing σ_8 from 0.933 ± 0.006 (G_5 with $\sum m_\nu = 0$) to 0.75 ± 0.02 (G_5 with $\sum m_\nu \neq 0$, independent of the hierarchy). For this reason, introducing massive neutrinos in CG cosmology has the effect of alleviating the CMB-WL tension [58].

In Fig. 5 we show the deviation of the best fit CMB TT power spectra, in units of TT variance, $\sigma_\ell = \sqrt{2/(2\ell+1)}C_\ell^{\Lambda\mathrm{CDM}}$, for each CG model, computed with respect to ΛCDM. In the upper panel we show the best fits from the analysis of PB, while in the lower one we show the results from PBHWS. As we can see, this deviation is larger in the case without massive neutrinos. We also see that there is almost no effect due to the hierarchy. Furthermore, we infer that G_3 always shows the worst

fit to the CMB data, overestimating the C_ℓ^{TT} at low ℓ, while in G_4 and G_5 the presence of extra parameters allows for a better fit. Nevertheless, when passing from G_4 to G_5, and thus allowing for a new free parameter (i.e. c_3), the fit does not look improved: in fact, we cannot see a substantial difference between the two cases, especially when looking at the full PBHWS data set results. We find that the choice of the hierarchy does not leave any signatures on the best fit of the matter power spectrum, as it is possible to grasp from the mean values obtained for σ_8 in the different cases.

Finally, we perform a complete statistical analysis, including the best chi squared and Bayesian evidence. In Table I, we show the values of the best fit χ^2 for the different runs and the Bayesian evidence factors ($\log_{10} B$), computed as defined in [18,59]. The last column is the difference between the Bayes factor of the ith CG model

TABLE I.   Values of the best fit χ^2 and of the Bayes factors ($\log_{10} B$) for the different CG models and data set combinations. The Bayes factors difference is computed with respect to the ΛCDM model assuming the same neutrinos scenario and the same data set. Negative values of the Bayes factor disfavor the CG model.

Model	Data set	χ^2	$\log_{10} B$	$\Delta \log_{10} B$
ΛCDM	PB	5635	-2459	0
ΛCDM + degenerate	PB	5635	-2459	0
ΛCDM + inverted	PB	5635	-2459	0
ΛCDM + normal	PB	5635	-2459	0
G_3	PB	5674	-2476	-17
G_3 + degenerate	PB	5646	-2463	-4
G_3 + inverted	PB	5646	-2463	-4
G_3 + normal	PB	5646	-2464	-5
G_4	PB	5667	-2474	-15
G_4 + degenerate	PB	5643	-2464	-5
G_4 + inverted	PB	5644	-2463	-4
G_4 + normal	PB	5645	-2463	-4
G_5	PB	5663	-2473	-14
G_5 + degenerate	PB	5644	-2465	-6
G_5 + inverted	PB	5644	-2465	-6
G_5 + normal	PB	5644	-2465	-6
ΛCDM	PBHWS	6020	-2628	0
ΛCDM + degenerate	PBHWS	6020	-2629	0
ΛCDM + inverted	PBHWS	6020	-2629	0
ΛCDM + normal	PBHWS	6020	-2629	0
G_3	PBHWS	6103	-2664	-36
G_3 + degenerate	PBHWS	6052	-2640	-11
G_3 + inverted	PBHWS	6048	-2640	-11
G_3 + normal	PBHWS	6047	-2640	-11
G_4	PBHWS	6078	-2652	-24
G_4 + degenerate	PBHWS	6035	-2635	-6
G_4 + inverted	PBHWS	6034	-2635	-6
G_4 + normal	PBHWS	6034	-2635	-6
G_5	PBHWS	6079	-2651	-23
G_5 + degenerate	PBHWS	6038	-2634	-5
G_5 + inverted	PBHWS	6036	-2634	-5
G_5 + normal	PBHWS	6038	-2635	-6

and the value obtained in the ΛCDM run, with the same hierarchy and data set. This value is interpreted following the Jeffreys scale that judges odds in favor of one model exceeding $100:1$, or $\Delta \log_{10} B > 2$, to be decisive in favor of the model. Looking at the G_3 best fits, we see that the $\Delta \log_{10} B$ decreases drastically in the runs without massive neutrinos. The situation gets better with massive neutrinos, but without showing any preference for a hierarchy. The same trend can also be noticed by looking at the right column in Table I. The $\Delta \log_{10} B < -4$ and the situation gets worse when the complete data set (PBHWS) is used ($\Delta \log_{10} B < -11$). This means that, for both data sets, G_3 is a worse fit to the data compared with ΛCDM. A similar result has been shown in Ref. [10], where the authors found that G_3 is effectively ruled out when constrained against ISW data. Compared to such an analysis, we use a different data set, which includes weak lensing, obtaining similar results. One would expect this situation to improve significantly in the G_4 and G_5 runs, since the presence of more parameters (ξ for G_4, ξ and c_3 for G_5) should give to the model more freedom to adapt to the data. However, these are not the cases and the differences in the $\log_{10} B$ exceed the 4 units, for both models with massive neutrinos regardless of the data set considered. Such differences in the Bayes factor exceed the 20 units in the scenarios with zero neutrino mass in the runs with the full data set. In summary, the higher Bayesian evidence is always found when fitting with ΛCDM, with no visible improvement when allowing the neutrino mass to vary and no effect coming from the hierarchy, regardless of the data set combination. Thus, the negative values of $\Delta \log_{10} B$ indicate that all the different CG models are strongly disfavored with respect to ΛCDM. Because such discrepancies in the $\log_{10} B$ comparison are very large, we consider our conclusion exhaustive and very robust.

In conclusion, we claim that all CG models are statistically ruled out by cosmological data. Thus, we confirm that the G3 model is excluded by data as previously noticed in Ref. [10]. More remarkably, the constraining power of the data sets used in this analysis allows us to exclude G4 and G5 as well, for the first time only by means of cosmological data. Interestingly this latter result is in line with the theoretical implications of the measurements of GW170817 and its electromagnetic counterpart which severely constrain both G4 and G5 [24–28].

V. CONCLUSION

In this work we have explored the phenomenology of covariant Galileons in light of the latest releases of cosmological data. For the first time in the literature CGs have been constrained against a wide and comprehensive data set, containing WL measurements from the KiDS Collaboration. As an additional degree of freedom of the theory, we have allowed for three different mass hierarchies and we have investigated the corresponding bounds on the CGs and cosmological parameters with current data. We have first considered three different CG classes, cubic (G_3), quartic (G_4) and quintic (G_5) Galileon in order to distinguish the effect of the different terms in the Lagrangian. Then for each of them, we have considered four different scenarios: a cosmology with $\Sigma m_\nu = 0$, and cosmologies with three different mass hierarchies, i.e. normal, inverted and degenerate. We have included for the same scenarios the ΛCDM model for comparison and actually distinguish the impact of the additional scalar field and that of massive neutrinos.

For the analysis presented in this work, we used two separate data sets as explained in Sec. III, but we did not find any significant improvement when comparing the results from PB (Planck + BAO) with the ones from the

TABLE II. Constraints on cosmological and model parameters at 1σ. These values are obtained through the analysis of the full PBHWS data set.

Model	σ_8	Ω_m	H_0	Σm_ν	ξ	c_3
ΛCDM	0.83 ± 0.01	0.298 ± 0.007	68.7 ± 0.5	$\cdots$	$\cdots$	$\cdots$
ΛCDM + degenerate	0.82 ± 0.02	0.300 ± 0.007	68.4 ± 0.6	0.08 ± 0.06	$\cdots$	$\cdots$
ΛCDM + inverted	0.82 ± 0.02	0.300 ± 0.007	68.4 ± 0.6	0.07 ± 0.06	$\cdots$	$\cdots$
ΛCDM + normal	0.82 ± 0.02	0.300 ± 0.007	68.4 ± 0.6	0.07 ± 0.06	$\cdots$	$\cdots$
G_3	0.928 ± 0.007	0.266 ± 0.004	74.6 ± 0.4	$\cdots$	$\cdots$	$\cdots$
G_3 + degenerate	0.72 ± 0.02	0.298 ± 0.007	70.3 ± 0.6	0.85 ± 0.08	$\cdots$	$\cdots$
G_3 + inverted	0.72 ± 0.02	0.297 ± 0.007	70.3 ± 0.6	0.85 ± 0.08	$\cdots$	$\cdots$
G_3 + normal	0.72 ± 0.02	0.298 ± 0.007	70.3 ± 0.6	0.85 ± 0.08	$\cdots$	$\cdots$
G_4	0.948 ± 0.008	0.264 ± 0.005	74.7 ± 0.5	$\cdots$	2.53 ± 0.06	$\cdots$
G_4 + degenerate	0.76 ± 0.02	0.293 ± 0.007	70.9 ± 0.6	0.80 ± 0.09	2.53 ± 0.07	$\cdots$
G_4 + inverted	0.76 ± 0.02	0.293 ± 0.007	70.9 ± 0.6	0.80 ± 0.09	2.53 ± 0.07	$\cdots$
G_4 + normal	0.76 ± 0.02	0.293 ± 0.007	71.0 ± 0.7	0.80 ± 0.09	2.53 ± 0.08	$\cdots$
G_5	0.933 ± 0.006	0.264 ± 0.005	74.7 ± 0.5	$\cdots$	2.23 ± 0.03	0.076 ± 0.006
G_5 + degenerate	0.76 ± 0.02	0.294 ± 0.006	70.9 ± 0.6	0.80 ± 0.09	2.24 ± 0.03	0.080 ± 0.001
G_5 + inverted	0.75 ± 0.02	0.294 ± 0.007	70.9 ± 0.7	0.81 ± 0.09	2.24 ± 0.02	0.0796 ± 0.0007
G_5 + normal	0.75 ± 0.02	0.292 ± 0.007	71.0 ± 0.6	0.81 ± 0.09	2.24 ± 0.02	0.079 ± 0.001

complete PBHWS (Planck $+$ BAO $+ H_0 +$ weak lensing $+$ supernovae) data set. Thus, we showed the results of the complete data set containing for the first time measurements from the weak gravitational lensing survey of KiDS.

We confirm that a CG cosmology implies a nonzero neutrino mass, with $\Sigma m_\nu = 0$ giving always a bad fit to data in G_3, G_4 and G_5; see Table I and Fig. 5. The value of the neutrino mass is higher than in ΛCDM: for the normal hierarchy we got 0.85 ± 0.08 eV for G_3, 0.80 ± 0.09 eV for G_4 and 0.81 ± 0.09 eV for G_5, while ΛCDM gives 0.07 ± 0.06 eV. In view of this relaxed bound, we find no sizable difference with the other mass hierarchies, indicating that current data cannot pick up the subtle features in the matter power spectrum due to the differences in the relativistic to nonrelativistic transition redshifts. When including massive neutrinos, the models considered seem to be really efficient in solving the CMB-low z tensions, by preferring a higher value of H_0 and lowering σ_8 (see Table II).

Nevertheless, a careful statistical analysis, based on the χ^2 and the Bayesian evidence comparison, shows that all the CG models are a much worse fit to the data, compared to ΛCDM, for whichever hierarchy is considered (see Table I), even the models, like G4 and G5, that have extra free parameters. The results of such a simple analysis are strong enough to confidently rule out all the CG models. In the case of G_3, this was already noticed in [10], where the authors found that the cubic Galileon is effectively ruled out by ISW data. From Fig. 5 we can see that, whichever CG configuration or hierarchy is used, the model always give a bad fit for the CMB TT power spectrum at low ℓ. We can see that including $\sum m_\nu \neq 0$ helps in lowering the χ^2 by a factor of 3, but still the $\Delta \log_{10} B$, computed with respect to ΛCDM, is large. These results allow us to claim for the first time that the entire class of CG models is statistically ruled out by cosmological data only.

Recently, in [24–28], it was shown that the measurements of the electromagnetic counterpart of the gravitational wave GW170817 [22,23] set stringent theoretical constraints on the quartic and quintic Lagrangians, practically ruling out their contribution from the action, unless they reduce to a standard conformal coupling. The cubic Galileon is not affected by these bounds. We have shown that cosmological data alone are able to exclude the viability of all CG models.

---

[1] C. Deffayet, G. Esposito-Farese, and A. Vikman, Phys. Rev. D **79**, 084003 (2009).

[2] G. W. Horndeski, Int. J. Theor. Phys. **10**, 363 (1974).

[3] C. Deffayet, S. Deser, and G. Esposito-Farese, Phys. Rev. D **80**, 064015 (2009).

[4] T. Kobayashi, M. Yamaguchi, and J. Yokoyama, Phys. Rev. Lett. **105**, 231302 (2010).

[5] C. Burrage, C. de Rham, D. Seery, and A. J. Tolley, J. Cosmol. Astropart. Phys. 01 (2011) 014.

[6] T. Kobayashi, M. Yamaguchi, and J. Yokoyama, Prog. Theor. Phys. **126**, 511 (2011).

[7] C. Deffayet, O. Pujolas, I. Sawicki, and A. Vikman, J. Cosmol. Astropart. Phys. 10 (2010) 026.

[8] A. Barreira, B. Li, C. M. Baugh, and S. Pascoli, J. Cosmol. Astropart. Phys. 11 (2013) 056.

[9] A. Barreira, B. Li, C. M. Baugh, and S. Pascoli, J. Cosmol. Astropart. Phys. 8 (2014) 059.

[10] J. Renk, M. Zumalacarregui, F. Montanari, and A. Barreira, J. Cosmol. Astropart. Phys. 10 (2017) 020.

[11] H. Hildebrandt *et al.*, Mon. Not. R. Astron. Soc. **465**, 1454 (2017).

[12] K. Kuijken *et al.*, Mon. Not. R. Astron. Soc. **454**, 3500 (2015).

[13] J. T. A. de Jong, G. A. V. Kleijn, K. H. Kuijken, and E. A. Valentijn (Astro-WISE, KiDS Collaborations), Exp. Astron. **35**, 25 (2013).

[14] S. Hannestad and T. Schwetz, J. Cosmol. Astropart. Phys. 11 (2016) 035.

[15] F. Simpson, R. Jimenez, C. Pena-Garay, and L. Verde, J. Cosmol. Astropart. Phys. 06 (2017) 029.

[16] S. Vagnozzi, E. Giusarma, O. Mena, K. Freese, M. Gerbino, S. Ho, and M. Lattanzi, Phys. Rev. D **96**, 123503 (2017).

[17] W. Yang, R. C. Nunes, S. Pan, and D. F. Mota, Phys. Rev. D **95**, 103522 (2017).

[18] F. De Bernardis, T. D. Kitching, A. Heavens, and A. Melchiorri, Phys. Rev. D **80**, 123509 (2009).

[19] T. M. C. Abbott *et al.* (DES Collaboration), arXiv:1708.01530.

[20] T. M. C. Abbott *et al.* (DES Collaboration), arXiv:1711.00403.

[21] B. P. Abbott *et al.* (Virgo, LIGO Scientific Collaborations), Phys. Rev. Lett. **119**, 161101 (2017).

[22] D. A. Coulter *et al.*, arXiv:1710.05452.

[23] B. P. Abbott *et al.*, Astrophys. J. **848**, L12 (2017).

[24] P. Creminelli and F. Vernizzi, Phys. Rev. Lett. **119**, 251302 (2017).

[25] J. M. Ezquiaga and M. Zumalacarregui, Phys. Rev. Lett. **119**, 251304 (2017).

[26] T. Baker, E. Bellini, P. G. Ferreira, M. Lagos, J. Noller, and I. Sawicki, Phys. Rev. Lett. **119**, 251301 (2017).

[27] J. Sakstein and B. Jain, Phys. Rev. Lett. **119**, 251303 (2017).

[28] D. Bettoni, J. M. Ezquiaga, K. Hinterbichler, and M. Zumalacarregui, Phys. Rev. D **95**, 084029 (2017).

[29] A. Nicolis, R. Rattazzi, and E. Trincherini, Phys. Rev. D **79**, 064036 (2009).

[30] M. Ostrogradsky, Mem. Acad. St. Petersbourg **6**, 385 (1850).

[31] A. De Felice and S. Tsujikawa, Phys. Rev. Lett. **105**, 111301 (2010).

[32] H. Mo, F. C. van den Bosch, and S. White, *Galaxy Formation and Evolution* (Cambridge University Press, Cambridge, UK, 2010).

[33] A. J. Cuesta, V. Niro, and L. Verde, Phys. Dark Universe **13**, 77 (2016).

[34] N. Palanque-Delabrouille *et al.*, J. Cosmol. Astropart. Phys. 11 (2015) 011.

[35] M. C. Gonzalez-Garcia, M. Maltoni, and T. Schwetz, J. High Energy Phys. 11 (2014) 052.

[36] B. Hu, M. Raveri, N. Frusciante, and A. Silvestri, Phys. Rev. D **89**, 103530 (2014).

[37] M. Raveri, B. Hu, N. Frusciante, and A. Silvestri, Phys. Rev. D **90**, 043513 (2014).

[38] G. Gubitosi, F. Piazza, and F. Vernizzi, J. Cosmol. Astropart. Phys. 02 (2013) 032.

[39] J. K. Bloomfield, E. E. Flanagan, M. Park, and S. Watson, J. Cosmol. Astropart. Phys. 08 (2013) 010.

[40] J. Gleyzes, D. Langlois, F. Piazza, and F. Vernizzi, J. Cosmol. Astropart. Phys. 08 (2013) 025.

[41] J. Bloomfield, J. Cosmol. Astropart. Phys. 12 (2013) 044.

[42] F. Piazza and F. Vernizzi, Classical Quantum Gravity **30**, 214007 (2013).

[43] N. Frusciante, M. Raveri, and A. Silvestri, J. Cosmol. Astropart. Phys. 02 (2014) 026.

[44] J. Gleyzes, D. Langlois, and F. Vernizzi, Int. J. Mod. Phys. D **23**, 1443010 (2014).

[45] A. Lewis, A. Challinor, and A. Lasenby, Astrophys. J. **538**, 473 (2000).

[46] A. Lewis and S. Bridle, Phys. Rev. D **66**, 103511 (2002).

[47] N. Frusciante, M. Raveri, D. Vernieri, B. Hu, and A. Silvestri, Phys. Dark Universe **13**, 7 (2016).

[48] N. Frusciante, G. Papadomanolakis, and A. Silvestri, J. Cosmol. Astropart. Phys. 07 (2016) 018.

[49] E. Bellini *et al.*, Phys. Rev. D **97**, 023520 (2018).

[50] N. Aghanim *et al.* (Planck Collaboration), Astron. Astrophys. **594**, A11 (2016).

[51] P. A. R. Ade *et al.* (Planck Collaboration), Astron. Astrophys. **594**, A13 (2016).

[52] S. Alam *et al.* (BOSS Collaboration), Mon. Not. R. Astron. Soc. **470**, 2617 (2017).

[53] A. G. Riess *et al.*, Astrophys. J. **826**, 56 (2016).

[54] S. Joudaki *et al.*, Mon. Not. R. Astron. Soc. **471**, 1259 (2017).

[55] M. Betoule *et al.* (SDSS Collaboration), Astron. Astrophys. **568**, A22 (2014).

[56] T. D. Kitching *et al.* (CFHTLenS Collaboration), Mon. Not. R. Astron. Soc. **442**, 1326 (2014).

[57] P. A. R. Ade *et al.* (Planck Collaboration), Astron. Astrophys. **594**, A14 (2016).

[58] A. Barreira, B. Li, C. Baugh, and S. Pascoli, J. Cosmol. Astropart. Phys. 08 (2014) 059.

[59] A. Heavens, Y. Fantaye, A. Mootoovaloo, H. Eggers, Z. Hosenie, S. Kroon, and E. Sellentin, arXiv:1704.03472.